Available online at www.eccomasproceedia.org
Eccomas Proceedia COMPDYN (2017) 3771-3778

ECCOMAS
Proceedia

COMPDYN 2017
6th ECCOMAS Thematic Conference on
Computational Methods in Structural Dynamics and Earthquake Engineering
M. Papadrakakis, M. Fragiadakis (eds.)
Rhodes Island, Greece, 15–17 June 2017

ON THE DYNAMIC BEHAVIOR OF A NONLINEAR OSCILLATOR WITH SOFTENING CHARACTERISTICS ATTACHED TO AN ELECTRO-DYNAMIC ACTUATOR

Alfonso Cutuli[1]**, Rosario Aiello**[1] **and Gianluca Gatti**[1]

[1] University of Calabria
Dept. of Mechanical, Energy and Management Eng., V. P. Bucci 46C, 87036 Rende, Italy
e-mail: alfonsocutuli@gmail.com, rio88_@hotmail.it, gianluca.gatti@unical.it

Keywords: Nonlinear Vibration, Nonlinear Oscillator, Vibration Control.

Abstract. *This paper presents an investigation on the dynamics involved in a two degrees of freedom system consisting of a nonlinear oscillator attached to the moving head of a linear electro-dynamic shaker. The effective stiffness of the nonlinear attachment is realized to achieve a softening force-deflection curve characteristics, and magnets are exploited to this purpose. The shaker is modelled as a linear spring-mass-damper system excited by a harmonic force with a varying excitation frequency. The attached oscillator consists of a cantilever beam with a specified mass on its tip, and it behaves linearly in the given domain of investigation. The nonlinearity is then introduced by adopting magnets in an attractive configuration acting on the tip of the beam. This has the twofold effect of reducing the linear effective stiffness and adding a negative stiffness of cubic type. The equations of motion of the system are presented, and an analytical solution in terms of amplitude-frequency equation is reported. This allows to explore the role of the key parameters involved in the system dynamics, and their effects is investigated in terms of the frequency response curve. The relationship among the non-dimensional, dimensional and physical parameters of an equivalent mechanical prototype is presented.*

Peer-review under responsibility of the organizing committee of COMPDYN 2017.
doi: 10.7712/120117.5683.17485

1 INTRODUCTION

The dynamics of two degree-of-freedom (DOF) nonlinear oscillators has been extensively reported in the literature, and the main applications have been related to the passive control of vibration, e.g. as vibration absorber [1] and energy sink [2].

A coupled system with springs of a linear-plus-cubic characteristics was investigated in [3], showing that the presence of the nonlinearity can result in amplification rather than reduction of the vibration amplitude. Reduction of the vibration amplitude can be obtained by a proper selection of the parameters in a system with nonlinear damping and nonlinear springs [4]. The theoretical investigation on the system behaviour in the vicinity of a main resonance was reported in [5], where possible quasi-periodic response was highlighted. In [6] such a nonlinear system was investigated for vibration mitigation and absorption, the local bifurcations of the periodic solutions was illustrated via frequency-response curves (FRCs), and their evolution with an increase of the excitation amplitude was shown. The performance and characteristics of a nonlinear neutralizer acting on a linear host structure were investigated in [7], and distinguishable features, such as closed detached resonance curves, have been predicted either inside [8] or outside [9,10] the main FRC. Experimental evidence of those features have been reported in [11,12]. In the majority of these studies, nonlinearity is concentrated on the suspension stiffness, which is modelled as a linear plus a cubic spring with a hardening characteristics. A static force-deflection curve of this type can be physically realized by assembling linear springs in a specific geometric configuration [12].

Other studies reported on the use of nonlinear springs with softening characteristics to achieve a quasi-zero stiffness effect for vibration isolation purposes [13-15]. The combination of mechanical springs and magnets has been exploited in [16].

In this paper we analyse an experimental setup in which an electro-dynamic shaker is used to excite a nonlinear system which has a much smaller mass than that of the shaker. The system is modelled as a nonlinear softening oscillator coupled to a linear system, representing the shaker, which also provide the harmonic force excitation. Because the system is softening, the resonance frequency due to the nonlinear system bends to lower frequencies and determines multi-valuedness of the amplitude response at some given frequencies of excitation. An analytical solution to the amplitude-frequency relation is reported, and a theoretical investigation on the effect of the system parameters on the response, has revealed coexisting steady-states regimes with detached resonance curves appearing inside the amplitude-frequency diagrams.

2 EXPERIMENTAL TEST-RIG

2.1 System description

The experimental test-rig under consideration in this work is illustrated in Fig. 1(a), and a schematic model is reported in Fig. 1(b). It consists of a large electro-dynamic shaker, on the moving head of which a support structure is attached. This is used to hold a cantilever beam, which is clamped at one extreme on the support and it is free to move at the other extreme. At the free end, two magnets are attached on each side of the beam and they act as a concentrated mass at the tip. They are also used to induce an auxiliary nonlinear stiffness component when they interact with their corresponding counter-parts on the support structure. If the magnets are arranged so that those on the tip of the beam are attracted by those on the support structure, the overall effect is to reduce the linear stiffness due to the slender beam alone, and add a nonlinear component of softening type. The physical parameters of the system and their corresponding values are reported in Table 1.

In the frequency range of interest, the beam with concentrated mass on its tip may be considered as a single DOF oscillator with effective stiffness and mass given by [17]

$$k_{1\_beam} = \frac{3EI}{L^3}$$
$$m = 0.2357 m_{beam} + m_{tip} \tag{1}$$

where I is the second moment of area of the beam section and m_{beam} is the beam mass.

Preliminary experimental tests were performed to estimate the frequency response function (FRF) of the system due to random excitation. An LMS Scadas III system was used for data acquisition and signal processing, and an accelerometer (PCB 352C22) was attached on the tip of the beam. Magnets on the support structure are removed so as to avoid any magnetic interaction with the beam, and the system was thus considered to behave as a two DOF linear oscillator. Result is reported in Fig. 2 as solid line and normalised to the maximum value. It can be seen that the resonance frequency at about 20 Hz due to the shaker is very highly damped, and the resonance frequency of the beam with attached tip mass is at about 34 Hz, as predicted by adopting the effective stiffness and mass in Eq. (1). To investigate the softening effect on the FRF, magnets are attached on the support structure in an attractive arrangement and at a specified distance, as reported in Table 1. It is reasonably assumed that the effect of the weight of the magnets on the mass of the excited main oscillator was negligible. The normalised result in this case is reported as dashed line in Fig. 2, where it can be noted that the overall effect, when using a linear FRF estimate, is to move the resonance peak to the lower frequencies, which is the case of a softening stiffness.

(a)

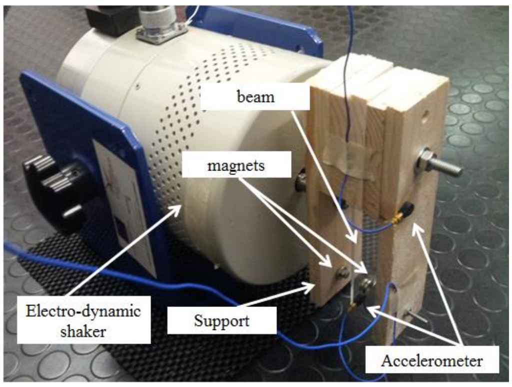

(b)

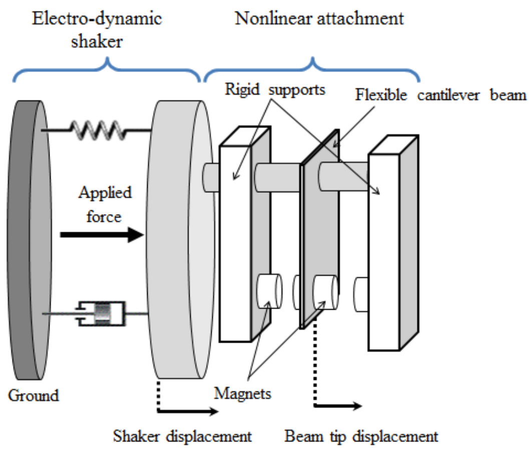

Figure 1. Two DOF system under study: (a) photograph and (b) schematic model.

Description	Parameter	Value	Description	Parameter	Value
Shaker stiffness [N/m]	k_{shaker}	9000	Beam width [mm]	a	30
Shaker moving mass [kg]	m_{shaker}	0.45	Beam thickness [mm]	s	2
Support mass [kg]	m_{supp}	0.15	Beam length [mm]	L	90
Magnet mass [g]	m_{mag}	1.2	Beam density [kg/m^3]	ρ	850
			Beam Young's modulus [N/m^2]	E	1.95e9
			Distance between magnets [mm]	b	10

Table 1: Physical parameters of the experimental system.

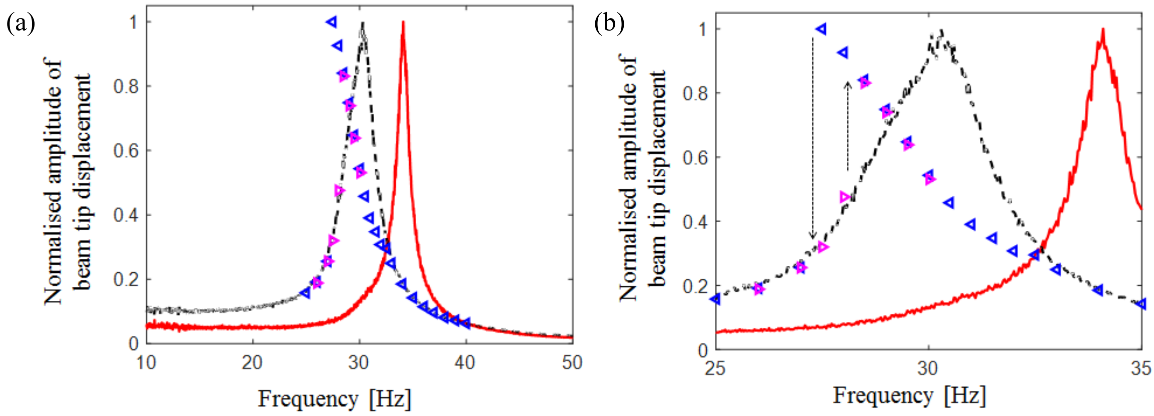

Figure 2. (a) Measured amplitude of beam tip displacement normalised to the maximum value, and (b) close-up. Linear FRF estimate without (solid line) and with (dashed line) magnets. Right (left) -pointing triangles indicate the FRC obtained by measuring the response at each frequency when increasing (decreasing) frequency of excitation.

For a better insight on the dynamic response of the system due to harmonic excitation, the shaker was driven with constant amplitude at each frequency, using a signal generator and a power amplifier. The system response in time was then measured using the accelerometer, and the spectrum of the corresponding signal was estimated by the frequency analyser. The amplitude of the spectrum at the excitation frequency is considered to reconstruct the frequency response curve (FRC), and this is normalised and plotted in Fig. 2 as well, using markers: left-pointing triangles are used to indicate the case where the excitation frequency is decreased from 40 to 25 Hz; right-pointing triangles indicate the case where the excitation frequency is increased from 25 to 30 Hz. Despite higher order harmonics were present around the resonance, it can be clearly noted that actual FRC presents a bending of the resonance peak to the lower frequencies, and this determines multi-valuedness and jump phenomena in the FRC. These latter are indicated in the close-up of Fig. 2(b) by vertical arrows pointing upwards for jump-up, or pointing downwards for jump-down.

2.2 Magnetic interaction

To quantify the magnetic interaction, an experimental setup, as illustrated in Fig. 3(a,b), was assembled and used to estimate the force-deflection characteristics. To this purpose, one magnet was constrained on a horizontal surface and a second magnet was attached on the base of a non-metallic cylinder, in such a way that it was set in a repelling arrangement to the previous magnet. A plastic tube was used to constrain the non-metallic cylinder to a vertical motion, when located on top of the magnet attached to ground. The force-deflection curve of magnetic interaction was then estimated by measuring the change in displacement for each additional weight applied on top of the non-metallic cylinder. Results of this test are reported in Fig. 3(c) as markers, and a fitting curve to the experimental data is also overlapped. A reasonably good fitting was achieved using the following equation

$$F_{mag} = \frac{C_{mag}}{y^n} \tag{2}$$

where $C_{mag} = 0.104$ Nm$^{1/3}$ and $n = 1/3$.

The total magnetic force acting on the tip of the beam is then given by the following relation

$$F_{mag\_tip} = -\frac{C_{mag}}{(b-z)^n} + \frac{C_{mag}}{(b+z)^n} \tag{3}$$

where b is given in Table 1, and $z = x_s - x$ is the relative displacement between the support, x_s, and the beam tip, x, as depicted in Fig. 4(a). Equation (3) may be expanded in McLaurin's series to the third order to give

$$F_{mag\_tip} \approx k_{1\_mag} z + k_{3\_mag} z^3 \tag{4}$$

where

$$\begin{aligned} k_{1\_mag} &= -2C_{mag} / 3b^{4/3} \\ k_{3\_mag} &= -28C_{mag} / 81b^{10/3} \end{aligned} \tag{5}$$

Equation (3) and (4) are plotted in Fig. 4(b), where it is noted that the cubic-type approximation in Eq. (4) (solid line) well approximates the expression in Eq. (3) (dashed line). The approximation is reasonable for relative displacements up to about half of the distance, b, between magnets at rest.

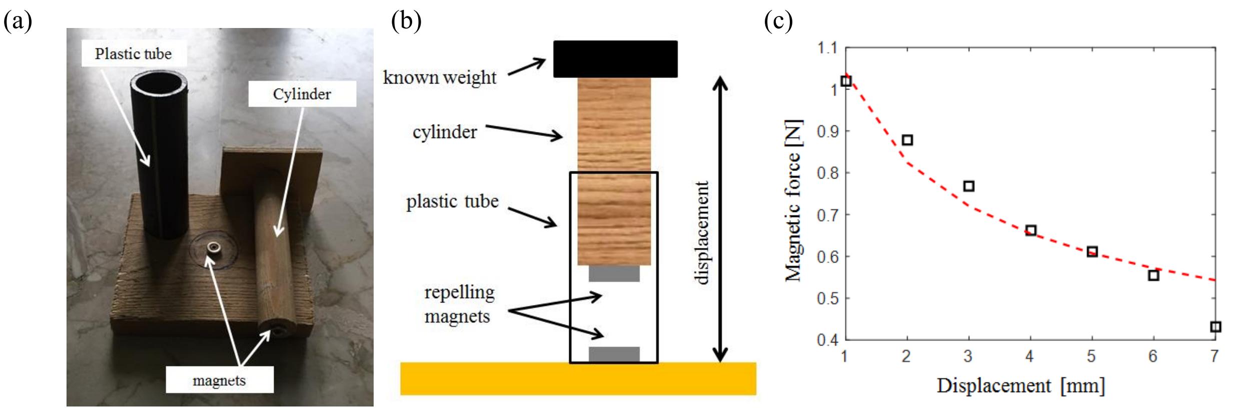

Figure 3. Experimental rig used to estimate the force-deflection curve characteristics of magnetic interaction: (a) photograph and (b) schematics. (c) Measured characteristics (markers) and fitting curve (dashed line).

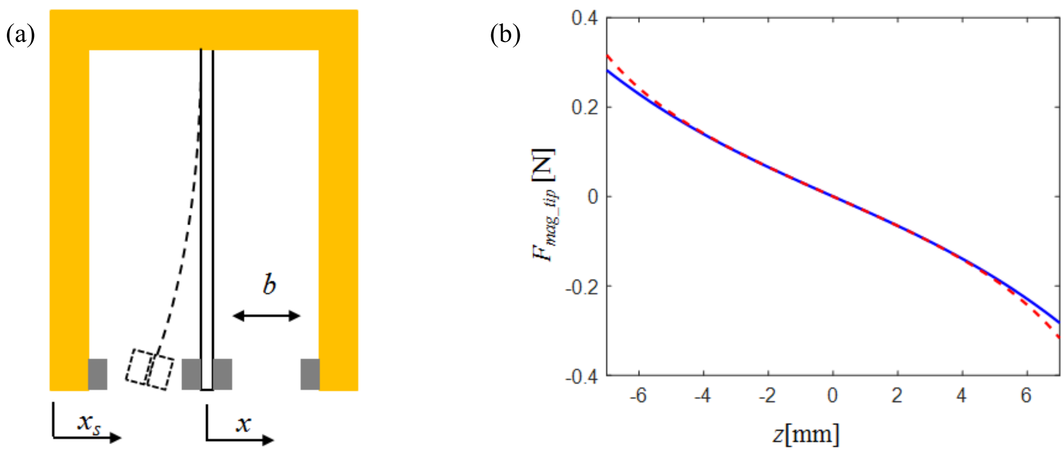

Figure 4. Magnetic force at tip: (a) close-up, (b) net force from Eq. (3) (dashed line) and Eq. (4) (solid line).

3 SYSTEM MODELLING

A simplified model for the system described in the previous section is reported in Fig. 5(a), and the corresponding equations of motion are given as

$$\begin{aligned} & m_s\ddot{x}_s + c_s\dot{x}_s + k_s x_s + c_1\dot{z} + k_1 z + k_3 z^3 = F\cos(\omega t) \\ & m\ddot{x}_s - m\ddot{z} - c_1\dot{z} - k_1 z - k_3 z^3 = 0 \end{aligned} \tag{6}$$

where parameters are indicated in Fig. 5(a). In particular it is

$$\begin{aligned} & k_1 = k_{1\_beam} + k_{1\_mag} = \frac{3EI}{L^3} - \frac{2C_{mag}}{3b^{4/3}} \\ & k_3 = k_{3\_mag} = -\frac{28C_{mag}}{81b^{10/3}} \end{aligned} \tag{7}$$

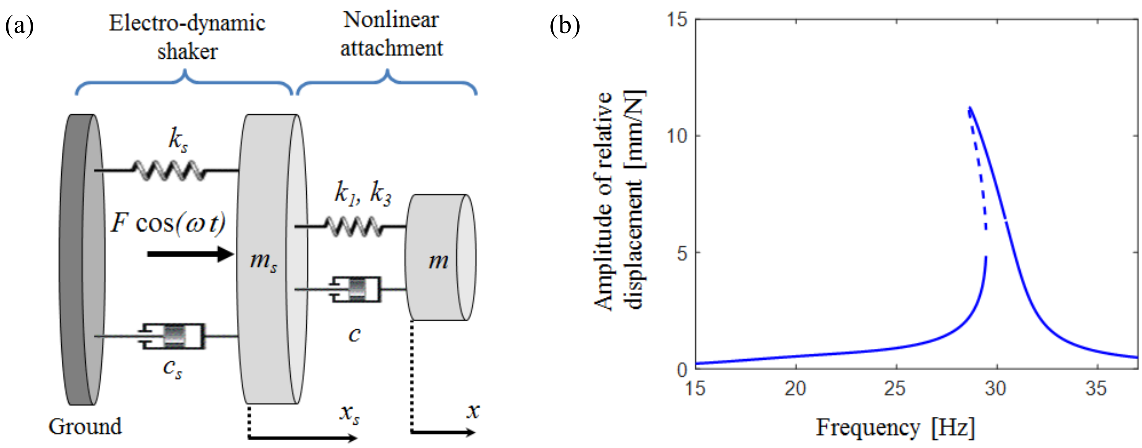

Figure 5. (a) Simplified model of the system in Fig. 1. (b) Example of FRC with stable (solid line) and unstable (dashed line) solutions.

In the assumption that the mass of the shaker and the attached support is much larger than the effective mass of the nonlinear oscillator, which is the actual case in Fig. 1, the non-dimensional form of Eqs. (6) simplifies to [10]

$$\begin{aligned} & y_s'' + 2\zeta_s y_s' + y_s = \cos(\Omega\tau) \\ & w'' + 2\zeta w' + \Omega_0^2 w + \gamma w^3 = y_s'' \end{aligned} \tag{8}$$

and the following non-dimensional parameters are defined

$$\begin{aligned} & y_s = \frac{x_s}{x_0},\ \ w = \frac{z}{x_0}, x_0 = \frac{F}{k_s}, \omega_s = \sqrt{\frac{k_s}{m_s}}, \omega_1 = \sqrt{\frac{k_1}{m}}, \tau = \omega_s t, \\ & \mu = \frac{m}{m_s}, \gamma = \frac{k_3}{\mu k_s}x_0^2, \zeta_s = \frac{c_s}{2m_s\omega_s}, \zeta = \frac{c}{2m\omega_s}, \Omega_0 = \frac{\omega_1}{\omega_s}, \Omega = \frac{\omega}{\omega_s} \end{aligned} \tag{9}$$

It is noted form Eq. (8) that the assumption of a small mass ratio, μ, implies that the shaker is not affected by the smaller nonlinear system, while this latter is affected by the former. A solution for the relative displacement amplitude in Eq. (8) is reported from [10] in terms of the amplitude-frequency response as

$$\frac{9}{16}\gamma^2 W^6+\frac{3}{2}\gamma W^4\left(\Omega_0^2-\Omega^2\right)+W^2\left(\Omega^4+4\zeta^2\Omega^2+\Omega_0^4-2\Omega_0^2\Omega^2\right)-\frac{\Omega^4}{\left(1-\Omega^2\right)^2+4\zeta_s^2\Omega^2}=0 \quad (10)$$

which is a cubic polynomial equation in terms of W^2 (i.e. the relative displacement amplitude squared), and thus admits three solutions, two of which are stable and one is unstable. The FRC of the relative displacement amplitude is plotted in Fig. 5(b) for the values of parameters listed in Table 1, assuming $\zeta = 0.02$, $\zeta_s = 0.3$ and $F = 4$ N. It can be noted that Fig. 5(b) qualitatively predicts a similar peak bending as that seen in the experimental results of Fig. 2.

The experimental case reported in this paper was particularly unfavourable, mainly due to the high damping of the shaker. In case of lighter damping, the FRC exhibits more interesting phenomena, such as resonance interactions and appearance of detached curves inside the main FRC. For a softening attachment, this happens because its resonance peak bends to the lower frequencies and interacts with the resonance peak due to the shaker with attached support, as can be seen in Fig. 6(a) and (b), where a damping ζ_s of 0.03 and 0.01 is used, respectively.

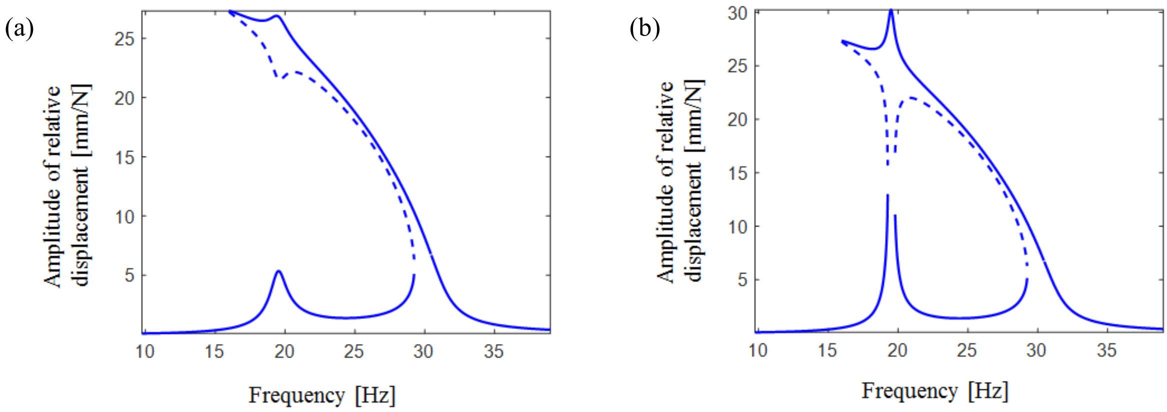

Figure 6. FRC when a light damping in the shaker is considered: (a) $\zeta_s = 0.03$, (b) $\zeta_s = 0.01$. Stable solutions (solid line) and unstable solutions (dashed line).

4 CONCLUSIONS

Based on the design and on some experimental tests performed on a nonlinear oscillator with softening spring characteristics driven by a shaker, this paper has shown some interesting dynamic effects appearing when the resonance peak of the nonlinear oscillator interacts with the resonance peak of the shaker: inner detached resonance curves manifest in the main frequency response curve for relatively light damping of the shaker. Although this was not shown experimentally due to the high damping of the actual shaker used in this work, the theoretical model predicts those features.

Understanding the complex dynamics involved in the type of system described in this paper, could be valuable not only for the tests of softening oscillators using an electro-dynamic shaker, but it could advance knowledge in the behaviour of two degrees of freedom nonlinear oscillators, and eventually foster pioneering engineering applications for vibration isolation, vibration absorption and vibration energy harvesting.

REFERENCES

[1] T. Detroux, G. Habib, L. Masset, G. Kerschen, Performance, robustness and sensitivity analysis of the nonlinear tuned vibration absorber. *Mechanical Systems and Signal Processing*, **60-61**, 799-809, 2015.

[2] Y. Starosvetsky, O.V. Gendelman, Vibration absorption in systems with a nonlinear energy sink: Nonlinear damping. *Journal of Sound and Vibration*, **324**, 916-939, 2009.

[3] J. Shaw, S.W. Shaw, A.G. Haddow, On the response of the non-linear vibration absorber. *International Journal of Non-linear Mechanics*, **24**, 281-293, 1989.

[4] S.J. Zhu, Y.F. Zheng, Y.M. Fu, Analysis of non-linear dynamics of a two-degree-of-freedom vibration system with non-linear damping and non-linear spring. *Journal of Sound and Vibration*, **271**, 15-24, 2004.

[5] O.V. Gendelman, E. Gourdon, C.H. Lamarque, Quasiperiodic energy pumping in coupled oscillators under periodic forcing. *Journal of Sound and Vibration*, **294**, 651-662, 2006.

[6] Y. Starosvetsky, O.V. Gendelman, Response regimes of linear oscillator coupled to nonlinear energy sink with harmonic forcing and frequency detuning. *Journal of Sound and Vibration*, **315**, 746-765, 2008.

[7] M.J. Brennan, G. Gatti, The characteristics of a nonlinear vibration neutralizer. *Journal of Sound and Vibration*, **331**, 3158-3171, 2012.

[8] G. Gatti, Uncovering inner detached resonance curves in coupled oscillators with nonlinearity. *Journal of Sound and Vibration*, **372**, 239-254, 2016.

[9] N.A. Alexander, F. Schilder, Exploring the performance of a nonlinear tuned mass damper. *Journal of Sound and Vibration*, **319**, 445-462, 2009.

[10] G. Gatti, M.J. Brennan, On the effects of system parameters on the response of a harmonically excited system consisting of weakly coupled nonlinear and linear oscillators. *Journal of Sound and Vibration*, **330**, 4538-4550, 2011.

[11] A.D. Shaw, T.L. Hill, S.A. Neild, M.I. Friswell, Periodic responses of a structure with 3:1 internal resonance. *Mechanical Systems and Signal Processing*, **81**, 19-34, 2016.

[12] G. Gatti, M.J. Brennan, Inner detached frequency response curves: an experimental study. *Journal of Sound and Vibration*, http://dx.doi.org/10.1016/j.jsv.2017.02.008.

[13] S.E. Woodard, J.M. Housner, Nonlinear behavior of a passive zero-spring-rate suspension system. *Journal of Guidance, Control, and Dynamics*, **14**, 84-89, 1991.

[14] P. Alabuzhev, A. Gritchin, L. Kim, G. Migirenko, V. Chon, P. Stepanov, *Vibration Protecting and Measuring Systems with Quasi-Zero Stiffness*, Hemisphere, New York, 1989.

[15] T. Mizuno, M. Takasaki, D. Kishita, K. Hirakawa, Vibration isolation system combining zero-power magnetic suspension with springs. *Control Engineering Practice*, **15**, 187-196, 2007.

[16] A. Carrella, M.J. Brennan, T.P Waters, K. Shin, On the design of a high-static–low-dynamic stiffness isolator using linear mechanical springs and magnets. *Journal of Sound and Vibration*, **315**, 712-720, 2008.

[17] S.S. Rao, *Mechanical Vibrations*, Prentice Hall, 2011.